Self organization of a hexagonal network of quasi-free-standing monolayer graphene nanoribbons

Y. Murata, M. Takamura, H. Kageshima, and H. Hibino

NTT Basic Research Laboratories, NTT Corporation, Atsugi, Kanagawa 243-0198, Japan

We investigated the H desorption process and the surface structure after H desorption in quasi-free-standing monolayer graphene (QFMLG) on silicon carbide (SiC). *In situ* scanning tunneling microscopy observations revealed that H adatoms preferentially desorb at SiC step edges. We found self-organization of a hexagonal network of QFMLG nanoribbons during H desorption. The surface structure on the nanoribbons indicates that electron scattering occurs at the boundary between the QFMLG and H-desorbed regions. The configuration of the network is determined by the formation energy of the boundary and by the surface stress energy.

I. INTRODUCTION

Graphene, a two-dimensional (2D) crystalline sheet of carbon,[1] has generated considerable attention owing to its ultrathin geometry and high carrier mobility,[2] with potential applications in high-performance low-power electronics[3] and as transparent electrodes.[4] In order to realize graphene devices, it is necessary to control the geometry and electronic structure. It has been shown that the band gap of graphene can be controlled when it is tailored into a ribbon shape with a width of up to several nanometers.[5] Some methods have been proposed to pattern graphene, such as lithography, unzipping of carbon nanotubes,[6] surface-assisted coupling of precursor molecule,[7] and electron-stimulated hydrogen desorption from graphene on silicon carbide (SiC) with a scanning tunneling microscope (STM) tip.[8] However, these methods do not satisfy the requirements for ideal nanoribbons in terms of production efficiency, uniformity of crystal orientation, and edge structure.

Riedl *et al.* have reported that H intercalation decouples a buffer layer from covalent bonds with a SiC substrate.[9,10] The decoupled buffer layer exhibits a band structure typical of graphene with less interaction from the SiC substrate.[11] Therefore, it is called quasi-free-standing monolayer graphene (QFMLG). The intercalated H atoms desorb by annealing in a vacuum and QFMLG partially transforms back into a buffer layer.[12,13] The buffer layer does not have the electronic properties of graphene due to covalent bonds with the SiC substrate.[14] For the fabrication of graphene nanostructures, it is desirable to create H-desorbed regions, i.e., electrically insulating regions, in QFMLG with arbitrary configurations and confine the in-plane shape of graphene. However, the H adsorption characteristics and the H desorption process in QFMLG are not fully understood. Therefore, we investigated the process of H desorption from QFMLG and the surface structure after H desorption with an STM. The activation energy for H desorption from QFMLG estimated by the *in situ* STM observation suggests that H adatoms diffuse at the graphene/SiC interface and desorb from the surface at SiC step edges. We found that during H desorption, a hexagonal network of QFMLG nanoribbons with armchair edges is self-organized. The surface structure on the nanoribbons indicates that electron scattering occurs at the boundary between the QFMLG and H-desorbed regions. The configuration of the network is determined to minimize the sum of the formation energy of the boundary between

the QFMLG and H-desorbed regions and the surface stress energy.

II. METHOD

An *n*-type $4H$-SiC(0001) substrate was used as a sample. The sample surface was etched in H_2 (25 Torr, 50 sccm) at 1500 °C for 5 min, annealed in Ar (600 Torr, 500 sccm) at 1650 °C for 5 min to form a buffer layer, and annealed in H_2 (85 Torr, 200 sccm) at 950 °C for 30 min for H intercalation. The sample cut to a size of 2×10 mm^2 was transferred to an ultrahigh vacuum (UHV) (1×10^{-10} Torr) chamber equipped with a variable-temperature STM (Omicron NanoTechnology) and degassed at 150 °C for 14 h. The sample temperature during STM observations was directly measured with an infrared pyrometer.

III. RESULTS

Figure 1 shows typical STM images of the sample at room temperature. The surface has terraces with a width of ∼1000 nm. A honeycomb structure with periodicity of ∼0.25 nm is observed on the terrace, confirming the successful formation of QFMLG [Fig. 1(b)]. Other features are hexagonal holes with a size of ∼100 nm and depth of ∼0.25 nm, which correspond to the height of a SiC bilayer [Fig. 1(a) inset]. The edges of the holes mainly have directions along SiC[11$\bar{2}$0]. It seems that the holes are formed by H etching of the SiC surface during H intercalation since they are not observed before the H_2 treatment. QFMLG is also formed inside the SiC holes and it covers the edges of the holes continuously [Fig. 1(b)].

We observed the surface structure after partial H desorption. The sample was annealed at 670 °C for 2 h in a vacuum. Figure 2(a), taken after cooling to 540 °C, shows that hexagonal patches with a size of ∼20 nm and rough corrugation appear around the upper edges of SiC holes. The magnified image at 590 °C in Fig. 2(b) and the line profile in Fig. 2(d) show that the patches have a surface structure with 6×6 periodicity of SiC (about 1.8 nm) and appear only at the upper edge of a SiC hole, not at the bottom edge. On the other hand, the honeycomb structure of graphene is still observed outside the patches in the magnified image at room temperature [Fig. 2(c)]. The patches are identified as the regions where intercalated H atoms desorbed and QFMLG was transformed back into a buffer layer by annealing in a vacuum.[15] Most of the sample
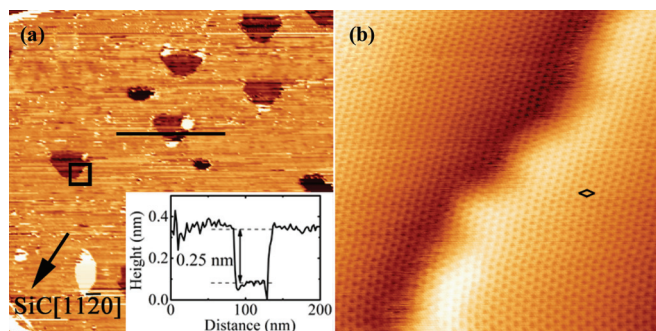
FIG. 1. (Color online) (a) STM image of a $4H$-SiC(0001) sample at room temperature after H intercalation (scan size = 500×500 nm^2, bias voltage = -0.14 V, tunnel current = 0.5 nA, height range = 0.66 nm). Inset: Line profile along the solid line. (b) Magnified image around the edge of a SiC hole indicated by a square in (a) (10×10 nm^2, -0.13 V, 0.6 nA, 0.41 nm). The left side of the image is inside the hole. A unit cell of graphene is indicated by the rhombus.

surface is still covered with QFMLG. The edges of H-desorbed patches have directions along SiC[11$\bar{2}$0], which correspond to armchair edges of QFMLG. Although the H-desorbed patches are also seen on a flat terrace far from the edges of SiC holes, the patches are few in number, in contrast to another report.[12]

We investigated the time evolution of the surface structure at 590–670 °C by *in situ* STM observation. Figure 3 shows H-desorbed patches around a SiC hole. At 590 °C

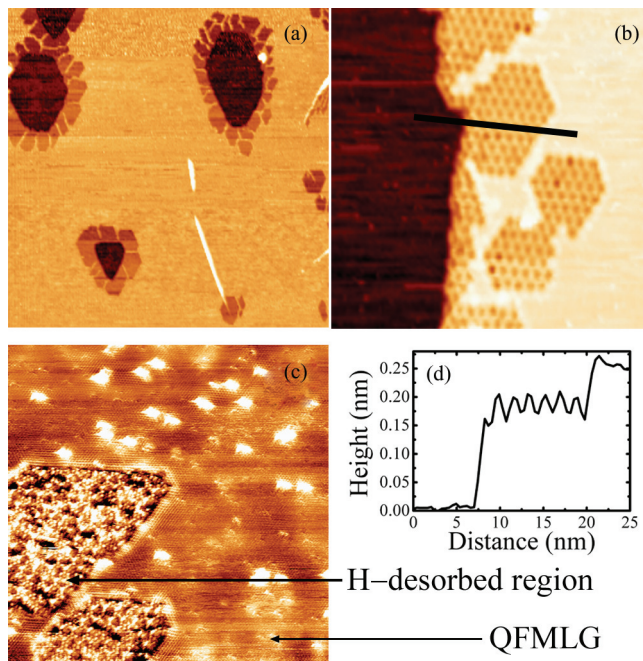FIG. 2. (Color online) (a) STM image at 540 °C after annealing at 670 °C for 2 h in a vacuum (500×500 nm^2, -0.14 V, 0.5 nA, 0.40 nm). (b) STM image at 590 °C around the edges of a SiC hole (50×50 nm^2, -0.14 V, 0.5 nA, 0.25 nm). The left side is inside the hole. (c) STM image of an H-desorbed patch at room temperature (50×50 nm^2, -0.13 V, 0.5 nA, 0.20 nm). (d) Line profile along the solid line in (b).

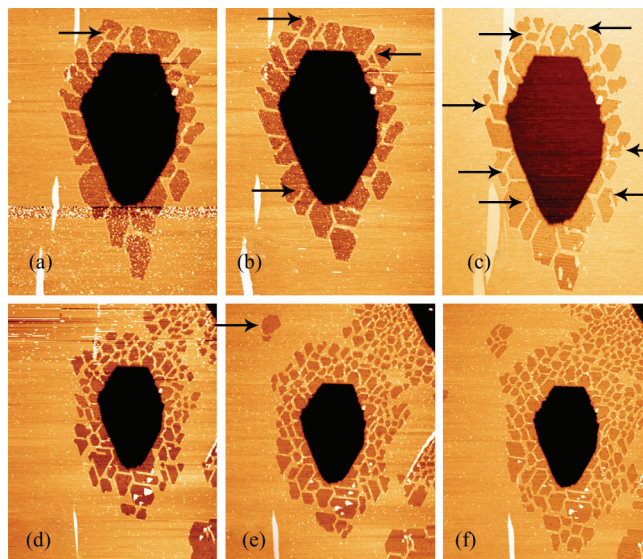

FIG. 3. (Color online) (a)–(c) Series of time-lapsed STM images at 590 °C, with elapsed times of (a) 0, (b) 10, and (c) 64 min. The arrows point to QFMLG nanoribbons intruding into H-desorbed patches (182×250 nm^2, -0.14 V, 0.5 nA, 0.25 nm). (d)–(f) Series of time-lapsed STM images at 630 °C, with elapsed times of (d) 0, (e) 37, and (f) 69 min. The arrow points to the nucleation of an H-desorbed patch on a flat terrace. There is a SiC step at the upper right corner (273×341 nm^2, -0.13 V, 0.5 nA, 0.25 nm).

[Figs. 3(a)–3(c)], although the net area of H-desorbed regions remains nearly unchanged with time, a QFMLG nanoribbon with a width of a few nanometers intrudes into a single H-desorbed patch along the SiC[11$\bar{2}$0] direction and the patch is split into several patches. At 630 °C [Figs. 3(d)–3(f)], the area of H-desorbed regions expands from SiC step edges, repeating the cycles in which each H-desorbed patch increases in size and is split into several patches by QFMLG nanoribbons. Nucleations of H-desorbed patches also take place occasionally on flat terraces far from SiC step edges [arrow in Fig. 3(e)]. Finally, H-desorbed patches separated by the network of QFMLG nanoribbons cover the entire surface. The morphology of the SiC substrate is not changed by annealing in a vacuum up to 670 °C.

The details of the surface structure after H desorption were investigated. Figure 4 shows STM images at room temperature taken after the observation in Fig. 3. A hexagonal network of QFMLG nanoribbons covers the entire surface. The average width and length of the QFMLG nanoribbons are a few nanometers and ~10 nm, respectively. The QFMLG nanoribbons run along the SiC[11$\bar{2}$0] direction, which corresponds to an armchair edge. In the magnified images at a three-way junction of QFMLG nanoribbons in Figs. 4(c)–4(e), a graphene $\sqrt{3} \times \sqrt{3}$-$R30°$ surface structure is observed throughout the nanoribbons. A similar surface structure has been seen in monolayer graphene on SiC and in graphite as a result of the characteristic electron scattering at armchair edges.[16–18] This result reveals that electron scattering occurs at the boundary between the QFMLG and H-desorbed regions, although the carbon layer is continuous along the boundary of the two regions.
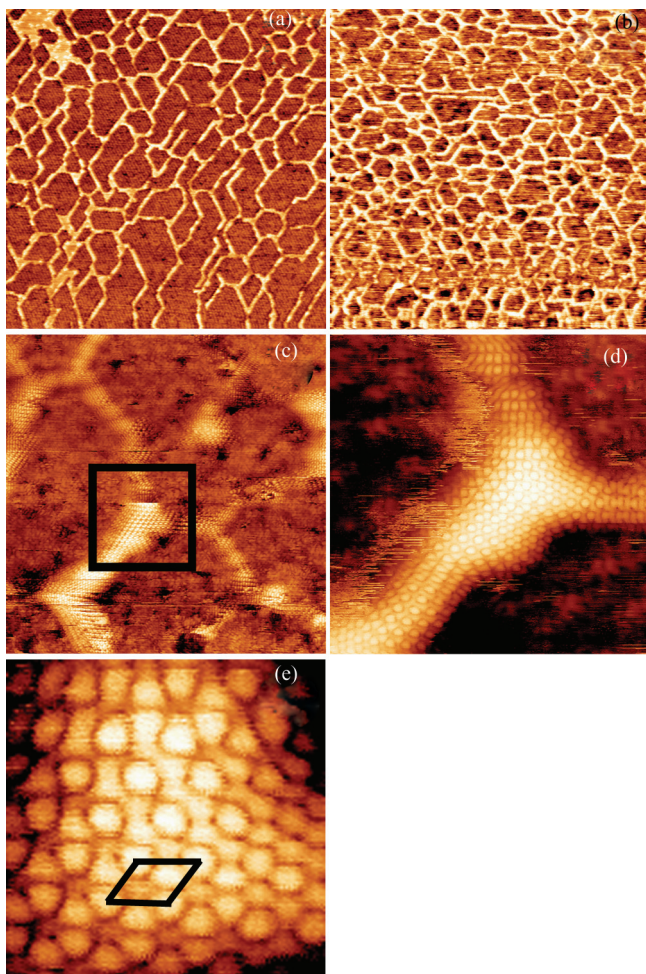
FIG. 4. (Color online) (a)–(c) STM images at room temperature after H desorption [(a) and (b) 200×200 nm², -0.002 V, 0.07 nA, 0.40 nm; (c) 30×30 nm², -0.002 V, 0.5 nA, 0.62 nm]. (d) Magnified image of the square in (c) (10×10 nm², -0.05 V, 0.5 nA, 0.52 nm). (e) Magnified image at the center of the nanoribbon in (d) (2.5×2.5 nm², -0.05 V, 0.5 nA, 0.46 nm). The rhombus shows a graphene $\sqrt{3} \times \sqrt{3}$-$R30°$ unit cell.

We next focus on the H desorption process. From the *in situ* observation of H desorption at 630, 650, and 670 °C, the time evolution of the coverage of the QFMLG region was measured. The coverage of the QFMLG region linearly decreases with time [Fig. 5(a)]. This indicates zero-order desorption; i.e., there is an equilibrium coexistence of 2D adatoms and a 2D solid phase.[19] The H desorption rates were estimated by straight line fits and plotted as a function of temperature in the Arrhenius graph [Fig. 5(b)]. The effective activation energy for H desorption from QFMLG is 2.5 ± 0.4 eV. The desorption process includes the breaking of the bonds between H and Si atoms and penetration of H atoms through a graphene sheet. The activation energy measured in our experiment is comparable to the Si-H bonding energy on Si(111)-1 × 1 (2.50 eV)[20] and the energy for penetration of an H atom through a graphene sheet to the interface with SiC (>2.55 eV).[21] The latter report also showed that the penetration energy is significantly reduced through defects, dislocations, grain boundaries, and edges of graphene, and H atoms can
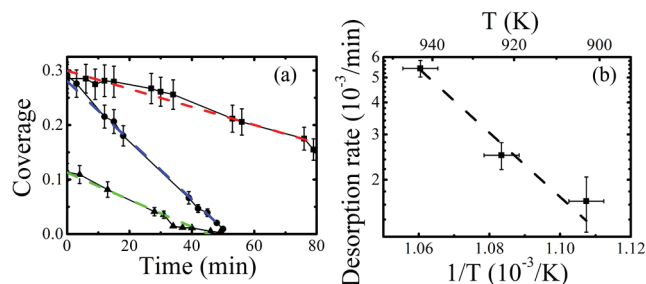

FIG. 5. (Color online) (a) Coverages of QFMLG regions at 630, 650, and 670 °C are plotted as squares, triangles, and circles as a function of time, with straight line fits as red, green, and blue dashed lines, respectively. (b) Arrhenius plot of desorption rates in (a).

diffuse at the graphene/SiC interface easily through the barrier with less than 0.67 eV. Therefore, H adatoms are not likely to simply penetrate through a graphene sheet at a flat terrace. The shape change of H-desorbed patches (Fig. 3) and the formation of more H-desorbed patches around the upper edges of SiC holes than on a flat terrace suggest that H adatoms diffuse at the graphene/SiC interface and desorb from the surface at SiC step edges, where it is easier for H adatoms to break the bonds with Si atoms or penetrate through a graphene sheet than at a flat terrace. Note that even at SiC step edges H adatoms need to penetrate through a graphene sheet when they desorb because SiC step edges are continuously covered by a graphene sheet [Fig. 1(b)]. This result is in contrast with another report, in which H desorption takes place mainly on a flat terrace above ~750 °C.[12] This contrast might be explained by the difference in the morphologies of SiC substrates. Many SiC holes in our sample may act as H desorption sites at a relatively low temperature of 630 °C.

The *in situ* observation of the H desorption process suggests that there is a stable configuration of QFMLG and H-desorbed regions. The STM images in Figs. 4(a) and 4(b) were taken at different locations on the sample after H desorption. In the two images, one can see differences in the average spacing and coverage of H-desorbed patches. The differences can be attributed to temperature variation or differences in circumstances, such as the existence of SiC steps and impurity particles. The average spacing λ and coverage θ of H-desorbed patches were measured at several locations and are plotted as squares in Fig. 6. When two different phases exist in the shape of hexagonal domains on a hexagonal-lattice surface as shown in the inset of Fig. 6, the spacing λ and coverage θ follow the equation below to minimize the sum of the formation energy of the boundary of the two phases and the surface stress energy in them:[22,23]

$$\lambda = \frac{2\pi a}{\sin(\pi \sqrt{\theta})} \exp\left(\frac{E_{wall}}{C} + 1\right), \quad C = \frac{1 - \upsilon}{2\pi \mu}(\sigma_1 - \sigma_2)^2.$$

(1)

Here, E_{wall}, σ_1, σ_2, a, υ, and μ are the formation energy of the boundary of the two phases per length, the surface stress tensors in the two phases, the lattice constant, Poisson's ratio, and bulk modulus, respectively. The experimental result is well fitted by the theory when $E_{wall}/C = 0.38$. Here, we used $a = 0.308$ nm for SiC. This result explains the shape change of a H-desorbed patch by intrusions of QFMLG nanoribbons
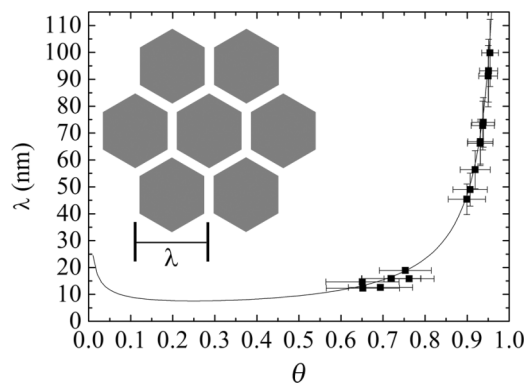
FIG. 6. Average spacings as a function of coverage of H-desorbed patches are plotted as squares. The solid curve is the minimum energy configuration of the model in the inset described by Eq. (1) when $E_{wall}/C = 0.38$.

at high temperature. The formation of the boundary is more energetically favored than the increase of the surface stress energy with increasing size of an H-desorbed patch. The difference in the interactions between graphene and the SiC substrate in the QFMLG and H-desorbed regions may give rise to the difference in the surface stress tensors in the two regions. In the H-desorbed region, the SiC substrate is compressively strained due to the lattice mismatch and the strong interaction with graphene. On the other hand, in the QFMLG region, graphene does not cause considerable stress on the SiC substrate due to the weak interaction (0.06 eV per C atom).[24]

Note that Eq. (1) was derived from a simple continuous model. Simply applying the Poisson's ratio and bulk modulus of graphene[25] in Eq. (1) to quantitatively evaluate the surface stress tensors and strains is not appropriate, since the real system comprising graphene and SiC is more complicated. We need further investigations of the structural properties in the real system, such as the Poisson's ratio, three-dimensional (3D) bulk modulus, and E_{wall}.

IV. CONCLUSION

We investigated the H desorption process and the surface structure after H desorption in QFMLG. The *in situ* STM observation showed that the H desorption process is zero-order desorption. The measured activation energy for H desorption suggests that H adatoms diffuse at the graphene/SiC interface and desorb from SiC step edges. We found self-organization of a hexagonal network of QFMLG nanoribbons with a width of a few nanometers and a length of ∼10 nm during H desorption. The nanoribbons have uniform armchair edges aligned with the crystal orientation of the SiC substrate. The graphene $\sqrt{3} \times \sqrt{3}$-$R30°$ surface structure on nanoribbons indicates that electron scattering occurs at the boundary between the QFMLG and H-desorbed regions. The configuration of the QFMLG and H-desorbed regions is determined by the formation energy of the boundary and the surface stress energy. These results point to the possibility of controlling the configuration of a network of QFMLG nanoribbons (width, spacing, and anisotropy) by applying an external strain on the substrate during H desorption.[26]

[1]A. K. Geim and K. S. Novoselov, Nat. Mater. **6**, 183 (2007).

[2]K. I. Bolotin, K. J. Sikes, Z. Jiang, M. Klima, G. Fundenberg, J. Hone, P. Kim, and H. L. Stormer, Solid State Commun. **146**, 351 (2008).

[3]A. K. Geim and A. H. MacDonald, Phys. Today **60**(8), 35 (2007).

[4]K. S. Kim, Y. Zhao, H. Jang, S. Y. Lee, J. M. Kim, K. S. Kim, J. H. Ahn, P. Kim, J. Y. Choi, and B. H. Hong, Nature (London) **457**, 706 (2009).

[5]M. Y. Han, B. Özyilmaz, Y. Zhang, and P. Kim, Phys. Rev. Lett. **98**, 206805 (2007).

[6]D. V. Kosynkin, A. L. Higginbotham, A. Sinitskii, J. R. Lomeda, A. Dimiev, B. K. Price, and J. M. Tour, Nature (London) **458**, 872 (2009).

[7]J. Cai, P. Ruffieux, R. Jaafar, M. Bieri, T. Braun, S. Blankenburg, M. Muoth, A. P. Seitsonen, M. Saleh, X. Feng, K. Müllen, and R. Fasel, Nature (London) **466**, 470 (2010).

[8]P. Sessi, J. R. Guest, M. Bode, and N. P. Gusisinger, Nano Lett. **9**, 4343 (2009).

[9]C. Riedl, C. Coletti, T. Iwasaki, A. A. Zakharov, and U. Starke, Phys. Rev. Lett. **103**, 246804 (2009).

[10]C. Riedl, C. Coletti, and U. Starke, J. Phys. D: Appl. Phys. **43**, 374009 (2010).

[11]F. Speck, J. Jobst, F. Fromm, M. Ostler, D. Waldmann, M. Hundhausen, H. B. Weber, and Th. Seyller, Appl. Phys. Lett. **99**, 122106 (2011).

[12]S. Forti, K. V. Emtsev, C. Coletti, A. A. Zakharov, C. Riedl, and U. Starke, Phys. Rev. B **84**, 125449 (2011).

[13]S. Watcharinyanon, C. Virojanadara, J. R. Osiecki, A. A. Zakharov, R. Yakimova, R. I. G. Uhrberg, and L. I. Johansson, Surf. Sci. **605**, 1662 (2011).

[14]K. V. Emtsev, F. Speck, Th. Seyller, L. Ley, and J. D. Riley, Phys. Rev. B **77**, 155303 (2008).

[15]C. Riedl, U. Starke, J. Bernhardt, M. Franke, and K. Heinz, Phys. Rev. B **76**, 245406 (2007).

[16]K. I. Sakai, K. Takai, K. I. Fukui, T. Nakanishi, and T. Enoki, Phys. Rev. B **81**, 235417 (2010).

[17]H. Yang, A. J. Mayne, M. Boucherit, G. Comtet, G. Dujardin, and Y. Kuk, Nano Lett. **10**, 943 (2010).

[18]A. Mahmood, P. Mallet, and J.-Y. Veuillen, Nanotechnology **23**, 055706 (2012).

[19]G. Le Lay, M. Manneville, and R. Kern, Surf. Sci. **65**, 261 (1977).

[20]X. M. Zheng and P. V. Smith, Surf. Sci. **282**, 173 (1993).

[21]A. Markevich, R. Jones, S. Öberg, M. J. Rayson, J. P. Goss, and P. R. Briddon, Phys. Rev. B **86**, 045453 (2012).

[22]H. J. W. Zandvliet, B. S. Swartzentruber, W. Wulfhekel, B. J. Hattink, and B. Poelsema, Phys. Rev. B **57**, R6803 (1998).

[23]P. Zeppenfeld, M. Krzyzowski, C. Romainczyk, G. Comsa, and M. G. Lagally, Phys. Rev. Lett. **72**, 2737 (1994).

[24]I. Deretzis and A. La Magna, Phys. Rev. B **84**, 235426 (2011).

[25]A. Politano, A. R. Marino, D. Campi, D. Farías, R. Miranda, and G. Chiarello, Carbon **50**, 4903 (2012).

[26]O. L. Alerhand, D. Vanderbilt, R. D. Meade, and J. D. Joannopoulos, Phys. Rev. Lett. **61**, 1973 (1988).